RESEARCH PAPERS

Response of hot wire anemometer probes to a stream of air bubbles in a water flow

K Bremhorst and D B Gilmore
Department of Mechanical Engineering, University of
Queensland, St Lucia 4067, Australia

Abstract The response of a hot wire anemometer in
bubbly two-phase air–water flow was studied in order to
establish the various processes taking place. For the
conventional hot wire design and operation at low overheat,
it was found that the sensor does not enter the bubble
completely, thus making measurements inside the bubble
virtually impossible. This is due to a liquid film which
attaches to the wire. For small bubbles it results in splitting
of the bubble into two separate ones except at low
velocities. Three types of interactions are identified –
direct, glancing and partial hits. Direct and glancing hits
result in identical signal level changes and hence
discrimination between bubble and no-bubble signals,
whereas partial hits give considerably reduced signal level
changes. Application of such measurements to determination
of local void fraction by use of signal probability density
plots is also considered.

1 Introduction

Measurement techniques in bubbly two-phase flow have
already been studied extensively and reported by Hsu *et al*
(1963), Delhaye (1969) and Herringe and Davis (1974), where
the emphasis has been directed towards the determination of
local void fraction and mean phase velocity. For measure-
ments in an electrically conducting fluid Herringe and Davis
(1974) found the single point resistivity probe to be most
suitable except at high void fractions where a two-needle
probe was found more satisfactory. When the liquid is not an
electrical conductor they concluded that the hot wire probe is
the most promising but give few details of the response of such
a probe in a two-phase flow. More details of the response of a
probe of the hot wire type are given by Hsu *et al* (1963) and
Delhaye (1969). Both attempt to clarify the physical processes
involved by the application of photographic techniques when a
vapour bubble flows past such a probe. Unfortunately, neither
gives a satisfactory explanation of the physical processes for all
stages of the probe–fluid interaction. Thus if it were desired to
measure turbulence levels of the liquid and the vapour phases
so that the effect of one phase on the other can be determined,
as suggested by Hsu *et al* (1963), it would be necessary for the
probe to pass through the liquid–vapour interface cleanly.
That this is not generally the case is readily seen from Herringe

and Davis (1974) who had to make allowance for the signifi-
cant response time to phase changes by a somewhat arbitrary
manipulation of signal probability density distributions to
correct for the finite time required for the liquid to run off the
sensor as it enters the gas phase.

Clearly, if more detailed flow measurements are to be
attempted than the now relatively well established measure-
ments of void fraction and phase velocity, a better under-
standing of the interfacial processes taking place is required.
This is particularly important if the phases are not in tempera-
ture equilibrium, in which case it is desired to pierce the
bubbles with a sensor to obtain instantaneous velocity and
temperature information of the gaseous phase. For such
applications the hot wire anemometer would be ideal as it
responds to both these stimuli.

The physical processes involved as bubbly two-phase flow
passes over a hot wire probe were examined and are reported
below. Only the case where the sensor temperature is well
below the saturation temperature of the liquid is considered.

2 Interaction between a hot wire probe and an air–water interface

As a bubble approaches and then passes over a hot wire probe,
several processes take place. Those in the purely liquid or
purely gaseous phase are well documented, including the
effects encountered when the bubble has a greater or lower
velocity than the liquid medium – refer to Hsu *et al* (1963)
and Delhaye (1969). Little is known, however, once the probe
interacts with the liquid–vapour interface when entering the
bubble and again when leaving the bubble. These two pro-
cesses are dominated by surface tension forces. In view of the
similarity between a hot wire probe and the wire frame com-
monly used for the measurement of surface tension it is
appropriate to commence with a full description of the wire
frame method or 'Bügelmethode' of surface tension measure-
ment described in detail by Lenard (1924).† It will be seen
from subsequent work that this gives an excellent insight into
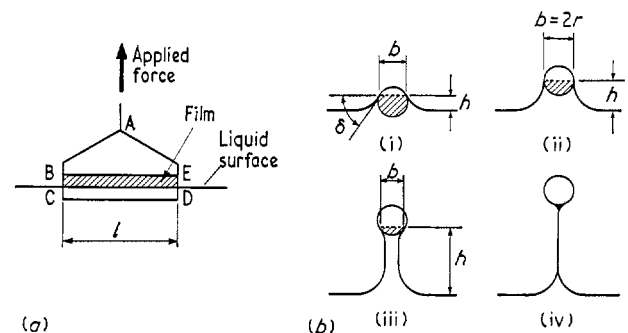the physical processes encountered as a hot wire enters a gas or
vapour bubble.

Figure 1 (*a*) Wire frame used by Lenard: (*b*) cross section
of wire–liquid interface

Figure 1(*a*) shows the wire frame used by Lenard for the
measurement of surface tension. A wire frame ABCDE is
attached to a spring balance. It carries stretched between B and
E the measuring wire of length *l* with which the liquid skin
(shaded area) is pulled out of the horizontal liquid surface. If
P is the downward force exerted by the skin, the surface

---

† The authors are most grateful to Dr F Durst, Sonderforsch-
ungsbereich 80, Universität Karlsruhe, Karlsruhe, West
Germany, for drawing their attention to this publication.

tension σ is given approximately by $P/2l$ when the diameter of the measuring wire BE is infinitely small.

For measuring wires of finite diameter $2r$, as is the case with hot wire probes, allowances must be made for the weight of liquid suspended beneath the measuring wire. In terms of the symbols of figure 1(b), this equals $(hlb\gamma - G)$ where γ is the specific weight of the liquid, and G is the weight of liquid displaced by the shaded section. In addition, the force due to surface tension must be resolved in the vertical direction. Thus,

$$P = 2\sigma l \sin \delta + hlb\gamma - G. \tag{1}$$

The force P is therefore a function of the variables h and δ. As h increases from zero, P increases until $\delta = 90°$ as shown in figure 1(b)(ii). In this case, which occurs at $h = a = \sqrt{(2\sigma/\gamma)}$, $\sin \delta$ is at its maximum, so that the first term of equation (1) is at its maximum.

For not excessively thick wires, the first term is much larger than the other two so that at $h = a$, P is close to its maximum value. As h is increased further, P decreases again since $\delta > 90°$ (figure 1(b)(iii)). When δ is so large that the two liquid surfaces meet, the case of figure 1(b)(iv) is obtained. For this case, equation (1) no longer holds since the liquid within the skin is no longer at rest. Instead, the liquid slowly runs down under the influence of its weight until the skin is so thin that it breaks. During this latter stage the force P increases almost to the value of the previous maximum. It is seen that during this process of withdrawal of the wire frame from the liquid, two force maxima are formed which are separated by a minimum. However, an important difference between these two maxima exists. The first maximum is one of equilibrium and can be maintained for any length of time, but the second one is only of very short duration and depends on the rate of liquid drainage.

It is of interest to calculate the height h for the first maximum, since this must be obtained as a very minimum attachment length for the liquid film which attaches itself to such a geometry when traversed from liquid to gas.

Taking $\sigma_{\text{water-air}} = 0.0725$ N m^{-1} at 20 °C and $\gamma_{\text{water}} = 9807$ N m^{-3}, it follows that $h = a = 3.85$ mm. Thus it must be expected that for sufficiently low velocity, as a hot wire enters an air bubble carried in a water flow, the water film will remain attached to the wire for at least this distance. The distance from $h = a$ until the film breaks will depend on the dynamics of the water skin and the velocity of the air relative to the air–water interface. Naturally, some deviation from this result must be expected, depending on the detailed construction of the wire supports, the wire straightness, whether or not it is perfectly wetted by the water along its whole length, and in the case of the hot wire the difference in temperature between the wire and the water and the effect of increased wire diameter at the ends due to plating commonly used.

3 Static interfacial piercing tests

A hot wire as shown in figure 2 was mounted on a vertical holder in a micrometer screw operated slider mechanism. By this means the wire could be traversed very slowly or in a stepwise fashion from air through the air–water interface while being observed under a microscope. This simulated the wire's piercing action of the bubble somewhat inaccurately for the motion from water to air since in the real flow the prongs would be the last to emerge from the liquid, whereas in this simulation the wire was effectively withdrawn from the water with no part of the prongs still in the water. In terms of figure 1(a) this means that Lenard's experiment was simulated without the sides BC and ED. The effect of this for a sufficiently long wire (in this case the length to diameter ratio is 117 excluding the plated ends) is to reduce the height of the wire above the undisturbed water level at which film breakage will
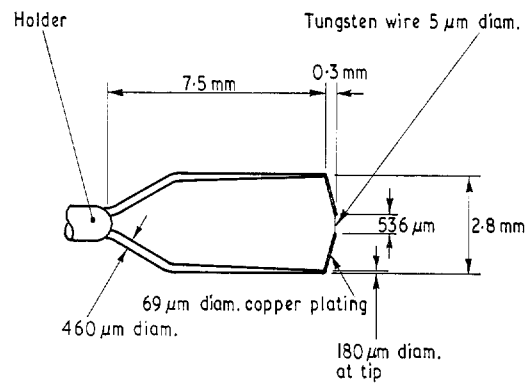

Figure 2 Hot wire probe details

occur. This was considered unimportant in view of the resultant simplicity and reduced disturbance to the free surface of the water, particularly, in the dynamic tests described in §4. The wire also had to be positioned forward of the prongs as shown in figure 2 to stop the water surface from forming a meniscus on the prongs first, which immediately jumps across the hot wire thus giving a completely false reading.

For the tests described below the hot wire was operated at a constant resistance ratio of 1·1 (overheat ratio = 0·1) resulting in a difference between mean wire temperature and water or air temperature of 20 °C, the water temperature at all times being equal to the air temperature. The results of a stepwise withdrawal from and reinsertion into the water are shown in figure 3. Water conductivity was sufficiently low so that the
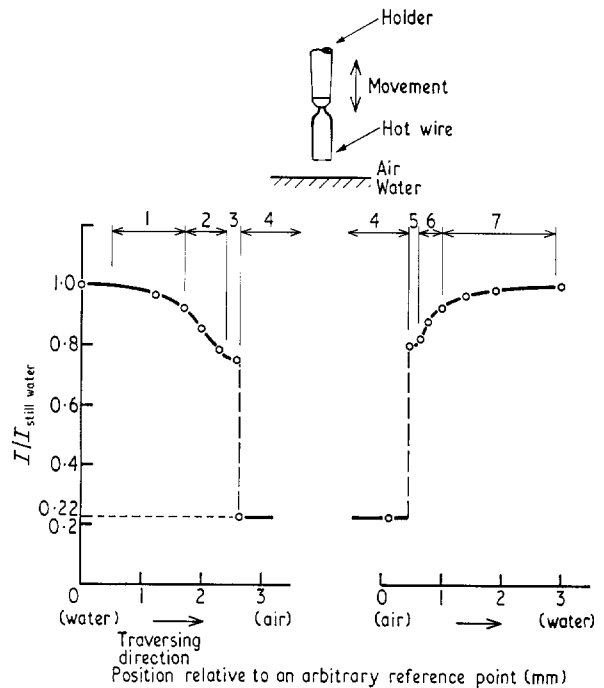

Figure 3 Static interfacial piercing test results

wire current changed by less than 0·1 % when water surrounded the wire supports but not the wire itself, thus making the short circuiting effect negligible.

Moving the wire from water to air, the water surface is raised whilst a water film remains around the wire (region 1, figure 3). This proximity to the interface gives a decrease in

heat transfer from the wire on the air side and hence a decrease in wire current. This decrease continues as the wire is withdrawn from the water until the water film stretched over the top of the wire breaks and a meniscus attaches to the wire. The meniscus then slides around the wire exposing more and more of its circumference to the air (region 2). A point is reached past which a further withdrawal of the wire produces very little change in wire current and hence heat transfer, indicating that the circumferential area in contact with the water remains unchanged (region 3). Further withdrawal leads to breakage of the film with a resultant change in heat transfer to that in air alone (region 4).

Regions 1 (part only), 2 and 3 together give the film breakage length of interest for two-phase flow measurements. In this case it is approximately 1·5–2 mm which, as expected, is less than the minimum of 3·85 mm calculated from Lenard's result in §2. For the arrangement where the hot wire is followed through the interface by the prongs the film breakage length will exceed 2 mm.

The reverse action of traversing the wire from air to water produces regions 4 to 7. As the wire approaches the water surface, the meniscus attaches to the wire suddenly (region 5). The wire can then be lowered somewhat without greatly altering the heat transfer (and hence wire current). This is followed by the water film attaching completely over the wire as it is traversed further into the elastic interface (region 6) until it becomes completely immersed in the water, resulting in the still water heat transfer level being reached (region 7). For this operation it is required that the wire approaches the water surfaces ahead of the prongs, otherwise the interface attaches to the prongs, jumps across the wire and in one operation covers the wire with water even when the wire is still above the surrounding water level.

4 Dynamic interfacial piercing test

The static tests described above give insight into the basic processes taking place as a hot wire pierces the air–water interface under essentially static or equilibrium conditions. In bubbly two-phase flow, the interface moves rapidly past the wire resulting in significant dynamic effects. To simulate these and establish how they alter the static results, the above experiments were repeated but with the wire moving through the interface at a finite velocity rather than in a slow stepwise fashion. Results obtained are shown in figure 4 for two different velocities.

Consider the test performed at 0·39 m s^{-1}. As the wire moves from water to air, the signal level drops sharply from that corresponding to 0·39 m s^{-1} in water until a short levelling out of the signal occurs. This corresponds to the state where a thin film of water is stretched over the wire and moves with it, thus giving a signal level corresponding to still water with a reduction in signal level due to the reduced heat transfer through this thin layer (region 1, figure 4). When the water film breaks over the top of the wire a meniscus attaches to the sides (region 2). During this process the heat transfer rate increases momentarily due to the relative velocity between the breaking water film and the wire. As the meniscus is formed on the wire sides, the signal drops below the first level section of the signal, the new level corresponding to exposure partly to air and partly to water. This step is an essential difference between the static and dynamic cases.

After the meniscus has formed on the wire sides, similar characteristics to the static test are displayed. The signal remains steady for a short time before dropping steeply to the air level as the film becomes detached from the wire (region 3). The signal then takes a considerable period (in this case one second) to reach the final air level (region 4). This is thought to
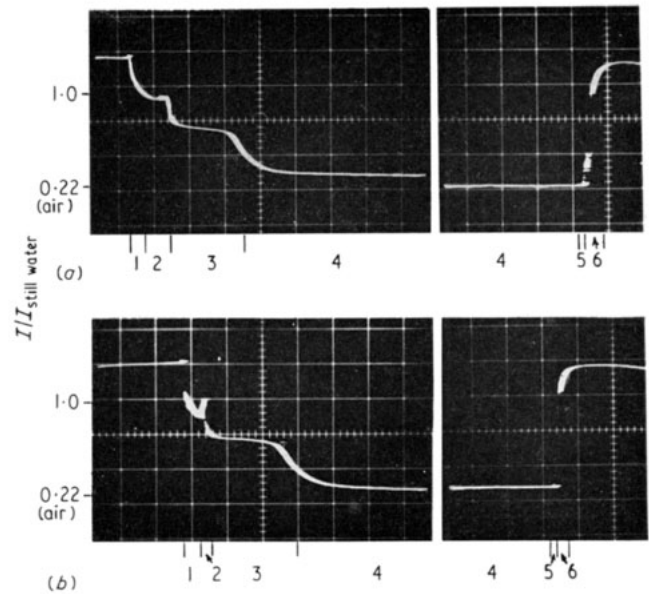

Figure 4 Dynamic interfacial piercing test results. Film breakage length $\simeq 6$ mm. Probe velocity = (a) 0·39 m s^{-1}, (b) 1·22 m s^{-1}. (5 ms/div)

be due to minute quantities of water remaining on the wire which require this time to reach the wire temperature and slowly evaporate from the wire after which the signal will return to the air level. The very abrupt step obtained during the static tests is therefore no longer present. The other major difference between the static and dynamic tests is that whereas for the former the film breakage length was 1·5–2 mm, for the latter it is just over 6 mm. This will be increased even further for the normal situation where the prongs follow the wire through the interface as already explained for the static tests. Breakage of the water film can therefore not be certain as a hot wire passes through a bubble with the result that the air level may never be reached.

As the wire is moved from air to water the signal level rises very sharply to the original level corresponding to a wire velocity of 0·39 m s^{-1} in water (region 6). Only a very slight levelling of the signal was noticeable as the water meniscus attached to the sides of the wire (region 5). At the higher piercing velocity (figure 4) similar results were obtained with region 5 being almost non-existent.

It is noteworthy that the signal characteristics obtained are very similar to those by Hsu et al (1963) which were obtained
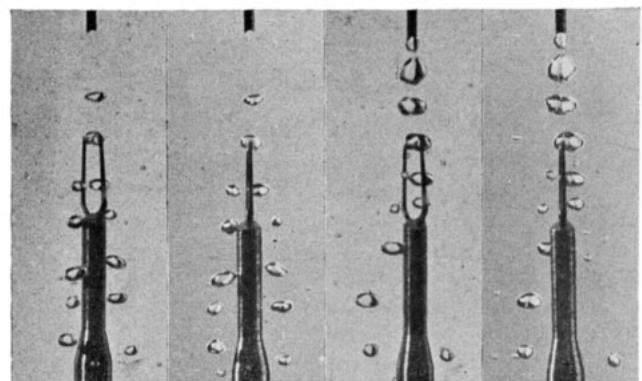

Figure 5 Single frame stereo photographs of probe–bubble interaction. Average bubble diameter = 1·5 mm. Bubble velocity = 1·1 m s^{-1}

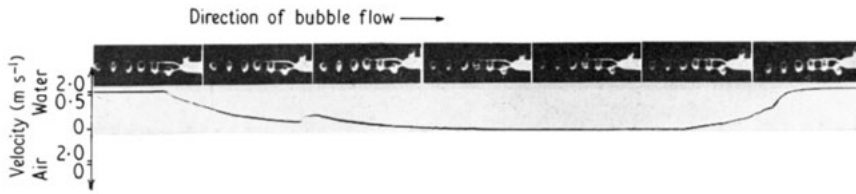Direction of bubble flow →

Figure 6 Simultaneous bubble–wire and electrical signal photographs

with a hot film anemometer, the tip of which was arranged so as to form the first contact with the interface.

5 Hot wire in a bubbly two-phase flow

To obtain a further assessment of the hot wire performance, the test wire was mounted in a water tunnel into which was injected a single bubble stream upstream of the probe. Bubble size was varied from one test to the next, but in all cases only bubbles with diameters of 0·75 to 5·0 mm were used since bubbles of diameter much larger than the wire length can be expected to behave almost identically to those in the tests of §4 for which the bubble diameter is effectively infinite. Only single bubble streams were studied in order to minimize signal contributions due to bubble interaction and large scale liquid turbulence.

The test section was vertical with the hot wire probe facing upstream. Bubbles were injected at the pipe centre line at a point 52 pipe diameters from the entrance to the straight pipe, the water being supplied from a constant head tank. Single frame as well as high speed movie photographs were taken of the probe–bubble interaction. In each case simultaneous photographs at an angular spacing of 45° were obtained to show the action in two different views. Also, high speed photographs of a single probe–bubble view and simultaneous hot wire anemometer signal as displayed on an oscilloscope were taken so that the electrical signal could be directly correlated with the visual observation of probe–bubble interaction.

Typical of the single frame stereo photographs is figure 5 which shows the most important aspects uncovered by the present investigation. For bubble sizes of the order of or smaller than the length of hot wire, the bubble is cut into two separate bubbles for direct as well as for some of the glancing hits. Also, the mechanism producing this is clearly seen. The wire pushes the downstream side of the bubble without piercing it until it touches the upstream side of the bubble at which stage the wire simply acts to separate it into two bubbles.

Typical of the high speed movie runs of simultaneous side-by-side records of the wire–bubble interaction and the electrical signal (obtained by driving the *y* input to an oscilloscope with the anemometer signal and using a stationary time base) is figure 6, which was a highly repeatable pattern. From many thousands of feet of such films the results of wire–bubble interaction may be summarized as shown in figures 7(*a*) and (*b*) for bubbles of smaller and larger diameter than the total
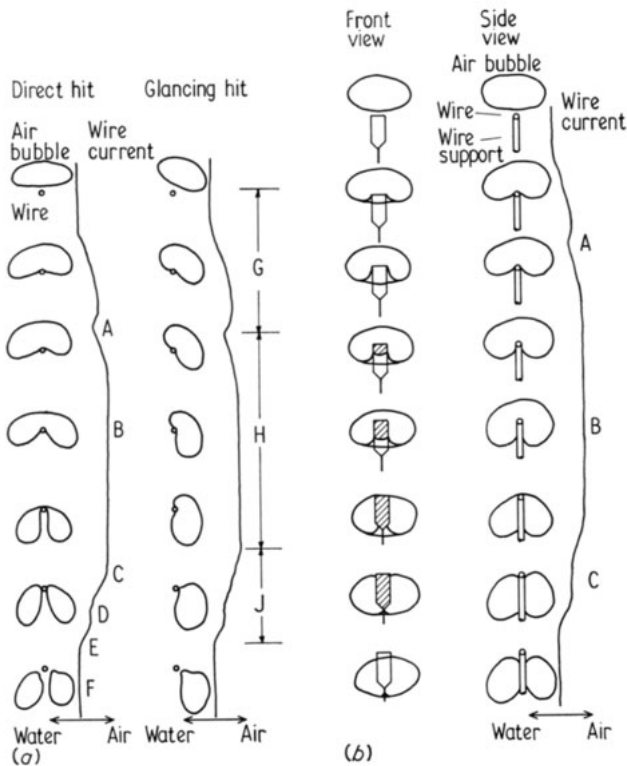

Figure 7 Summary of wire–bubble interaction.

(*a*) Bubble diameter smaller than total length. A: film braeks over top of wire; B: signal rises to the level corresponding to a meniscus attached to wire sides; C: approximate other side of bubble; D: signal is irregular as the wire touches opposite side of bubble; E: meniscus detaches reluctantly from wire; F: signal at water level; bubbles may or may not recombine; G: this section of signal identical to that for direct hits; H: this signal length is reduced for glancing hits; J: bubble stretching takes place in this region.

(*b*) Bubble diameter ≃ 5 mm (larger than total wire length). A: film breaks over top of wire; B: film attached to underside of wire; C: water film attached between supports and wire
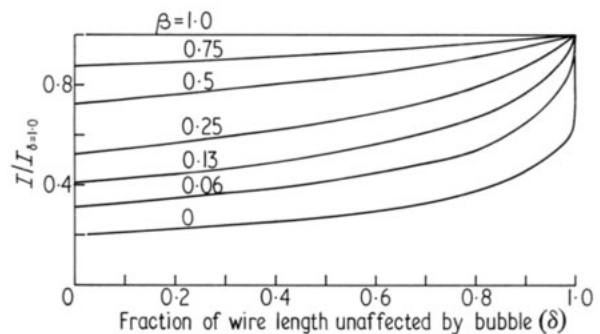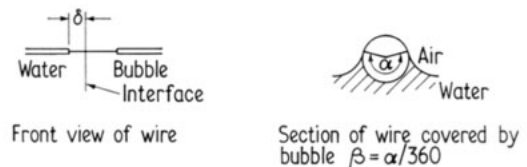

Figure 8 Calculated hot wire output for various wire–bubble interactions. Wire temperature = 40°C; fluid temperature = 20°C (5 μm tungsten wire, fluid at rest relative to wire)
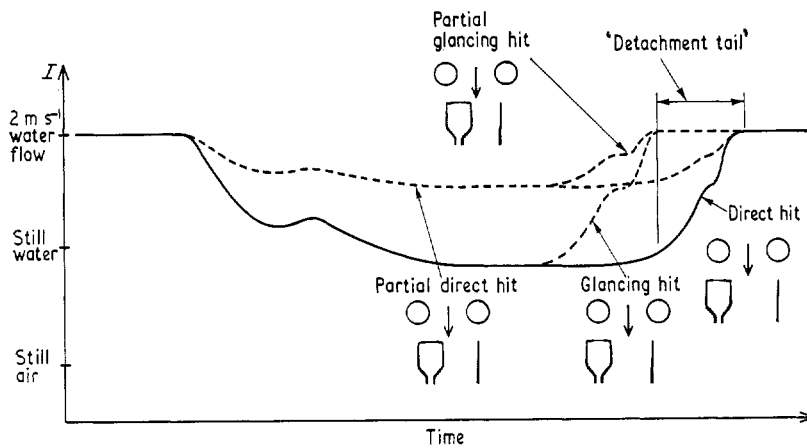
Figure 9(a) Signals obtained with identical bubbles for various types of hits
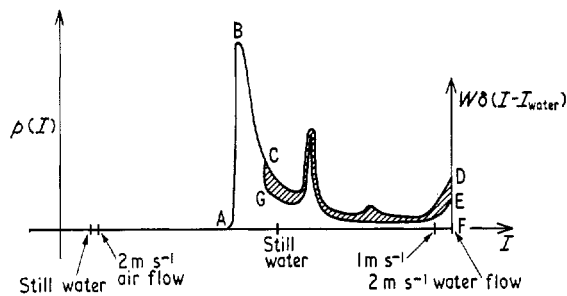

Figure 9(b) Probability density plot of hot wire signal for a stream of identical bubbles resulting in direct hits as shown in figure 9(a) (shaded area due to 'detachment tail').
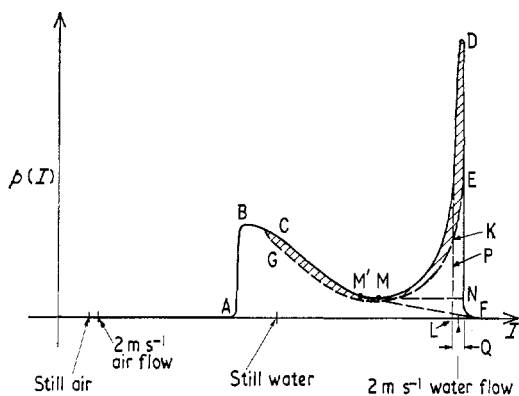$\int_{ABCDF} p(I)\, dI + W = 1.0$

Figure 9(c) Probability density plot of a signal train produced by a mixture of hits shown in figure 9(a). True local void fraction is given by an area between ABGKL and ABGKEF. P: lower limit for current above which liquid turbulence and bubble signals cannot be distinguished; Q: limits of I for 10% turbulence level in water.
$\int_{ABCDF} p(I)\, dI = 1.0$

wire length (including plated ends) respectively. A direct hit is classified as one affecting the whole length of the wire and for which the wire passes through the centre of the bubble, whereas for a glancing hit the whole wire length is still affected but the wire does not pass through the centre of the bubble. Full details of the results are given by Gilmore (1975).

The signals recorded by these means are in good agreement with those of the static and dynamic tests described above. For

the range of bubble sizes tested, the wire never pierced the bubble cleanly thus making measurements of the vapour properties inside the bubble impossible. Furthermore, the signal level reached while the meniscus was attached to the wire, during the wire's interaction with the bubble, rarely dropped much below that corresponding to the still water level which clearly indicates that the wire was never completely surrounded by air inside the bubble. This signal level is consistent with that reached in the near-flat portion of region 3 of the dynamic tests of figure 4. For bubble sizes much larger than 5 mm diameter – the largest tested here – the situation can be expected to be similar to the 5 mm diameter case. If the wire supports are sufficiently long and diameters are so large that the water film will break as indicated by Lenard's (1924) work, a signal as in region 4 of figure 4 will be obtained. At that stage such gross bubble distortion will, however, have taken place that measurements within the bubble would become meaningless.

The bubbly two-phase flow tests also revealed an additional signal characteristic not already found in the static and dynamic tests. During detachment of the bubble a definite levelling out of the wire current takes place just before the bubble finally breaks away from the wire. This is due to an affinity the bubbles have for attachment to the wire, particularly at low water velocities (1 m s⁻¹ and less). Because of this, the meniscus remains attached to the wire for as long as possible during the bubble's motion away from the wire, resulting in some stretching of the bubble. At the higher velocity tested (2 m s⁻¹) this was not significant. In subsequent discussions the section of the signal associated with this detachment phenomenon is referred to as the 'detachment tail' which cannot strictly be associated with the original undisturbed bubble. The other significant observation is that signal levels for direct and glancing hits are almost identical, the only difference being in the total length of signal obtained, such variations being due only to the length of signal at the 'air' level.

This then leads to a most important case, namely the partial hit which can be described as one affecting only part of the wire length. Letting δ be the fraction of wire length unaffected by the bubble and β the fraction of the affected portion's circumference covered by water, the results of figure 8 are obtained for constant mean wire temperature operation and a ratio of heat transfer coefficient of the wire in still water to that in still air of 23·9. These show that if the wire pierced the bubble cleanly, $\beta = 0$, excellent discrimination between air and water signals would be obtained even for quite large values of δ. From the current levels obtained for direct hits (for which $\delta = 0$) it can be deduced that values of β met in practice range

from 0·5 to 1·0, thus significantly reducing the discrimination which becomes almost proportional to the fraction of the wire length unaffected by the bubble. Thus for the case $\beta=0$, wire length is unimportant as even very small bubbles resulting in only a partial hit will give good discrimination, but for large β and bubble diameters smaller than the wire length, discrimination is reduced considerably. When the water has a finite rather than zero velocity the discrimination will be improved by the factor $(I_{\text{moving water}}/I_{\text{still water}})_{\delta=1}$.

6 Application of observations

Although the results of the previous sections show that measurements within bubbles are not possible with the probe tested, they can, however, be applied in the interpretation of probability density plots used to obtain local void fraction (Delhaye 1969 and Herringe and Davis 1974).

When a continuous stream of identical bubbles in a non-turbulent stream flows past the hot wire probe resulting in direct hits, a series of signals identical to those of figure 9(a) are obtained which have a probability density distribution as shown in figure 9(b) by the curve ABCDEF, where probability density is so defined that the area under this curve equals unity. The δ function is proportional to the time the wire is in water, whereas the area under the remaining curve (often taken as the local void fraction) is proportional to the time spent under the influence of the bubbles.

The effect of the 'detachment tail' is indicated by the shaded area. True local void fraction is then given by (area ABCDEF − shaded area CDEG). This ideal probability density plot will be altered significantly in a real flow, the most significant alteration being due to the partial hits. The effect due to varying bubble sizes will not be so significant as this only affects the time spent at the minimum level which is represented by the area under the $p(I)$ plot in the region A to B in figure 9(b). Liquid turbulence will also modify the result. Such a modified probability density plot is shown in figure 9(c) where a lower limit for the current is indicated above which liquid turbulence and bubble signals cannot be distinguished. A turbulence level of 10% was assumed in this figure resulting in velocity fluctuations of up to 33% of the mean velocity. The shaded area again represents the effect due to the 'detachment tail'. The local void fraction is now given by an area somewhere between areas ABGKL and ABGKEF. The extent of the difference between these two areas is determined by the liquid turbulence level.

The area for estimation of local void fraction used by Delhaye (1969) is given by area ABCMNF of figure 9(c) whereas that used by Herringe and Davis (1974) is ABCM′F. In the general case a discrepancy will exist between the various criteria but at high local void fractions the differences will become less significant.

The correct area to use lies between ABGKL and ABGKEF on figure 9(c) but this poses the practical problem of being able to determine the line GKE. At high fluid velocity (2 m s⁻¹ and above) the shaded area becomes negligible but increases with decreasing velocity. As the line GKE cannot be determined uniquely, calibration in a known flow appears to be the only reliable approach. Such a calibration would consist of measuring local void fraction in a homogeneous bubbly two-phase flow and comparing it with that obtained from the air and water flow rates. The difference between the two results would be due to the effect of the detachment tail and liquid turbulence.

7 Conclusions

For a hot wire probe, designed so that the active portion of the wire makes first contact with the water–air interface in bubbly two-phase flow and operated at a low overheat ratio so that the wire temperature is well below the saturation temperature of the fluid, it has been found that:
(i) as a bubble passes over the wire, a film attaches to the latter and does not detach for at least 5–6 mm of travel, which for hot wire probes of conventional proportions and bubbles of sufficiently large diameter will generally result in the film simply filling the space formed by the wire, its prongs and the probe holder with no resultant film detachment taking place;
(ii) for direct hits the bubbles are separated into two by the wire except for bubbles of significantly larger diameter than the total length of the hot wire (effective length plus plated ends if any);
(iii) for glancing hits the bubbles roll around the wire at low velocities but at higher velocities the bubbles are cut into two parts;
(iv) direct and glancing hits produce almost identical signal level changes, the only difference being in the length of the signal;
(v) partial hits give rise to a signal level change which decreases as the length of wire exposed to the bubble decreases;
(vi) the resultant electrical signal has a probability density distribution from which local void fraction can be estimated but the accuracy of this depends on the extent of the detachment tail and the liquid turbulence level. For accurate measurements, a calibration procedure in a known flow requires to be developed to account for these two effects.

References
Delhaye J M 1969 *Proc. 11th Nat. ASME/AICHE Heat Transfer Conf., Two Phase Flow Instrumentation, Minneapolis* (Minnesota: ASME) pp 58–69

Gilmore D B 1975 *M.Eng.Sc. Thesis* University of Queensland

Herringe R A and Davis M R 1974 *J. Phys. E: Sci. Instrum.* **7** 807–12

Hsu Y Y, Simon F F and Graham R W 1963 *Proc. ASME Multiphase Flow Symp., Philadelphia* (Minnesota: ASME) pp 26–34

Lenard P 1924 *Ann. Phys., Lpz* **74** 381–404